



ACADÉMIE  
DES SCIENCES  
INSTITUT DE FRANCE

# *Comptes Rendus*

---

## *Chimie*


Laura Iannazzo, Emmanuelle Braud, Matthieu Fonvielle  
and Mélanie Etheve-Quelquejeu

**Synthesis of RNA conjugates as bisubstrates for the study of transferases**

Volume 28 (2025), p. 111-129

Online since: 13 February 2025

<https://doi.org/10.5802/crchim.356>

 This article is licensed under the  
CREATIVE COMMONS ATTRIBUTION 4.0 INTERNATIONAL LICENSE.  
<http://creativecommons.org/licenses/by/4.0/>



*The Comptes Rendus. Chimie* are a member of the  
Mersenne Center for open scientific publishing  
[www.centre-mersenne.org](http://www.centre-mersenne.org) — e-ISSN : 1878-1543



Account

# Synthesis of RNA conjugates as bisubstrates for the study of transferases

Laura Iannazzo<sup>ⓧ, a</sup>, Emmanuelle Braud<sup>ⓧ, a</sup>, Matthieu Fonvielle<sup>ⓧ, b</sup> and  
Mélanie Etheve-Quellejeu<sup>ⓧ, \*, a, c</sup>

<sup>a</sup> Université Paris Cité, CNRS, Laboratoire de Chimie et Biochimie Pharmacologiques et Toxicologiques, F-75006 Paris, France

<sup>b</sup> Institute for Integrative Biology of the Cell (I2BC), CEA, CNRS, Université Paris-Saclay, Gif-sur-Yvette, France

<sup>c</sup> Institut Universitaire de France (IUF), France

*E-mails:* [laura.iannazzo@u-paris.fr](mailto:laura.iannazzo@u-paris.fr) (L. Iannazzo), [emmanuelle.braud@u-paris.fr](mailto:emmanuelle.braud@u-paris.fr) (E. Braud), [matthieu.fonvielle@i2bc.paris-saclay.fr](mailto:matthieu.fonvielle@i2bc.paris-saclay.fr) (M. Fonvielle), [melanie.etheve-quellejeu@u-paris.fr](mailto:melanie.etheve-quellejeu@u-paris.fr) (M. Etheve-Quellejeu)

**Abstract.** Bisubstrate compounds are designed to mimic the interaction of enzymes with their two natural substrates. These molecules contain two moieties mimicking the two substrates linked together by a covalent bridge, which enhances both selectivity and potency. This review shows the synthesis and utility of RNA conjugates, particularly peptidyl-RNA and cofactor-RNA conjugates, as bisubstrate analogues for studying two major families of RNA transferases: Fem aminoacyl transferases involved in bacterial cell wall synthesis and m<sup>6</sup>A methyltransferases, which catalyze RNA methylation. The synthetic routes developed to access the RNA conjugates cover nucleoside and nucleotide chemistry, site-specific RNA modifications, and solid phase synthesis or chemoenzymatic processes as well as strategies of oligonucleotide late-stage functionalization. The bisubstrate molecules have been used not only as inhibitors of these transferases but also as valuable chemical tools for elucidating enzyme mechanisms and facilitating structural studies.

**Keywords.** Bisubstrate, Aminoacyl transferases, RNA methyltransferases, Nucleoside chemistry, RNA conjugates.

**Funding.** CNRS, Paris Cité University, Agence Nationale de la Recherche, La Ligue contre le Cancer.

*Manuscript received 27 September 2024, revised and accepted 21 October 2024.*

## 1. Introduction

The bisubstrate strategy is recognized as a powerful approach for developing inhibitors and chemical tools to study enzyme function. This concept leverages the natural interaction of enzymes with multiple substrates to design molecules that can simultaneously engage more than one substrate-binding site. This approach often yields highly selective and potent inhibitors, with selectivity arising from targeting

two distinct binding sites and potency enhanced by the combined binding energies of both moieties and an entropy gain from a single molecule interaction. By designing molecules that mimic the interactions of both substrates, researchers can also create highly specific tools that provide insights into the enzyme mechanism of action. This dual engagement makes bisubstrate inhibitors valuable compounds for both therapeutic development and fundamental research.

Based on this concept, the bisubstrate molecules contain two units mimicking the two substrates attached together by a covalent linker (Figure 1). The linker, which is crucial for the correct binding and

\*Corresponding author

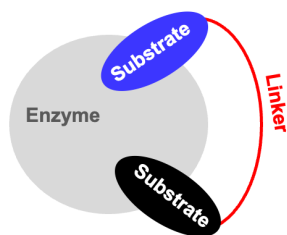


**Figure 1.** Bisubstrate-binding mode.

selectivity of the bisubstrate, must be optimized based on the distance between the two binding sites and the key residues involved in the catalytic pocket.

RNA-dependent enzymes, particularly those involved in RNA modifications or in non-ribosomal peptide synthesis, are especially amenable to bisubstrate strategies [1]. In this account, we focus on the use of bisubstrate strategies to explore two families of RNA-dependent enzymes: the Fem transferases and the m<sup>6</sup>A methyltransferases. We first explain the design of the bisubstrates, then describe their synthesis, and finally their use to explore the mechanism of the reaction catalyzed by the enzymes or as inhibitors of the transferases.

## 2. Peptidyl–RNA conjugates for the study of Fem transferases

### 2.1. The Fem transferases

Fem transferases are aminoacyl transferases that participate in peptidoglycan synthesis in Gram-positive bacteria. They catalyze the transfer of amino acids from aminoacyl-tRNA (aa-tRNA) to the amino group of L-Lys of peptidoglycan precursors (Scheme 1) [2,3]. Enzymes of the Fem family are attractive targets for the development of antibiotics active against resistant bacteria since the residues incorporated by the enzymes are essential for the last cross-linking step of peptidoglycan polymerization in several important  $\beta$ -lactam-resistant pathogens such as staphylococci, pneumococci, and streptococci [4]. Inhibiting Fem activity would therefore result in the production of incomplete precursors acting as chain terminators that block the formation of the essential peptidoglycan layer of the bacterial cell wall [5–7].

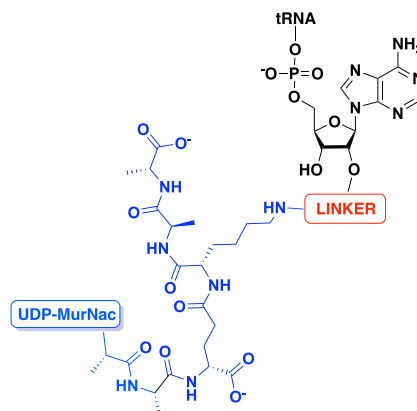


**Figure 2.** General structure of peptidyl–RNA conjugates to mimic the intermediate formed during the reaction catalyzed by FemX<sub>Wv</sub>.

In order to access chemical tools to achieve the resolution of the 3D structure of complexes comprising the enzyme and the aa-tRNA or to obtain inhibitors, the design and the synthesis of bisubstrates have been described for two Fem enzymes: FemX<sub>Wv</sub> [8,9] and FmhB [10] from *Weissella viridescens* and *Staphylococcus aureus*, respectively.

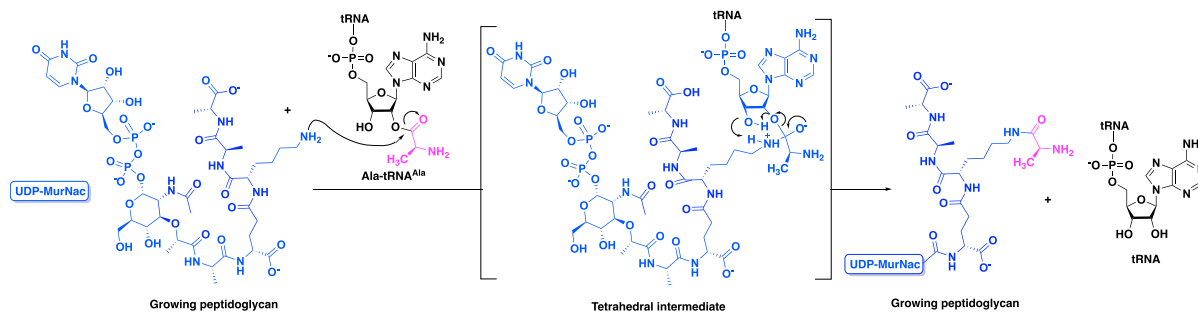
In *Weissella viridescens*, the transferase FemX<sub>Wv</sub> uses an ala-tRNA<sup>ala</sup> to transfer an alanine to a peptidoglycan fragment consisting of a pentapeptide tethered to a uridine diphosphate *N*-acetyl-muramic acid moiety [11] (UDP–MurNac) as described in Scheme 1.

To mimic the tetrahedral intermediate formed during the reaction catalyzed by FemX<sub>Wv</sub>, peptidyl–RNA conjugates were designed as bisubstrates. These compounds contain double-stranded RNA of different lengths simulating the natural substrate tRNA<sup>ala</sup> and a pentapeptide (L-Ala-D-iGlu-L-Lys-D-Ala-D-Ala) tethered to a UDP–MurNac to mimic the growing peptidoglycan (Figure 2). Linkers based on 1,2,3-triazole and squaramide were chosen to link the two units of the conjugates.

### 2.2. Synthesis of peptidyl–RNA conjugates

#### 2.2.1. Peptidyl–RNA conjugates with a triazole linker

**Synthesis of precursors.** Peptidyl–RNA conjugates containing a triazole linker as the bisubstrate of Fem transferases were first synthesized by Fonvielle et al.



**Scheme 1.** Mechanism of the transfer of Ala from Ala-tRNA<sup>Ala</sup> to the amino group of Lys at the C-3 position of peptidoglycan precursors catalyzed by the aminoacyl transferase FemX<sub>WV</sub> from *Weissella viridescens*.

in 2013 using the Cu(I)-catalyzed azide–alkyne cycloaddition (CuAAC) reaction [8]. The chemical strategy relies on the introduction of the azide function on the RNA moiety and the alkyne on the peptide mimicking the growing peptidoglycan.

The synthesis of 2'-azido-RNA helices was achieved using two routes, either by solid phase synthesis (SPS) to obtain a series of short azido-RNAs (18, 12, 10, and 8 nucleotides) or by a chemoenzymatic approach to prepare azido-RNAs of different sizes simulating the acceptor arm of the tRNA [8]. In this study, 2'-azido-adenosine derivatives **7a** and **7b** were synthesized in a seven-step procedure starting from commercially available adenosine **1** (Scheme 2) [8,9].

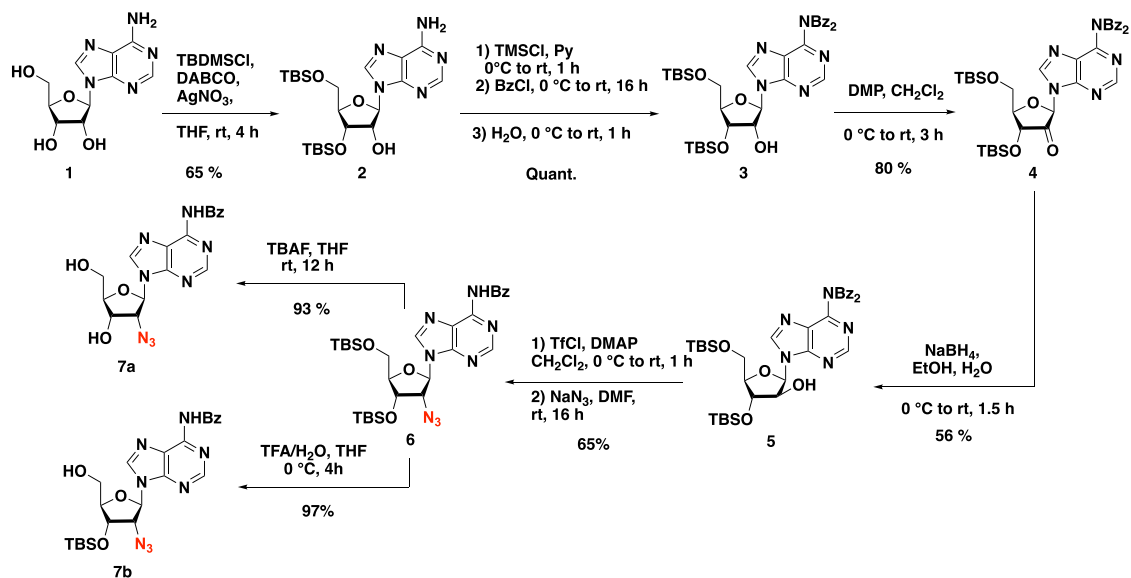
To achieve the synthesis of the short double-stranded azido-RNAs by SPS, 2'-azido-adenosine **7a** was first grafted on the resin via a succinyl linker, the resulting adenosine **8** being then engaged in SPS (Scheme 3, Route A). The strategy allows the introduction of a hexaethylene glycol linker to obtain stabilized short double-stranded azido-RNAs [9].

The use of a chemoenzymatic strategy was also investigated by Etheve-Quellejeu and coworkers to provide azido-RNA with increased size (Scheme 3, route B). The key step of such an approach is based on the synthesis of dinucleotide derivatives **12a–b** that were obtained by the phosphoramidite coupling between compound **7b** and the commercially available Ac-dC-PCNE and Ac-C-PCNE, respectively. Since the T4 RNA ligase recognizes 5'-phosphorylated RNAs, a chemical [3] and an enzymatic phosphorylation [12] were used to access 5'-phosphorylated 2'-azido-dinucleotides **13a** and

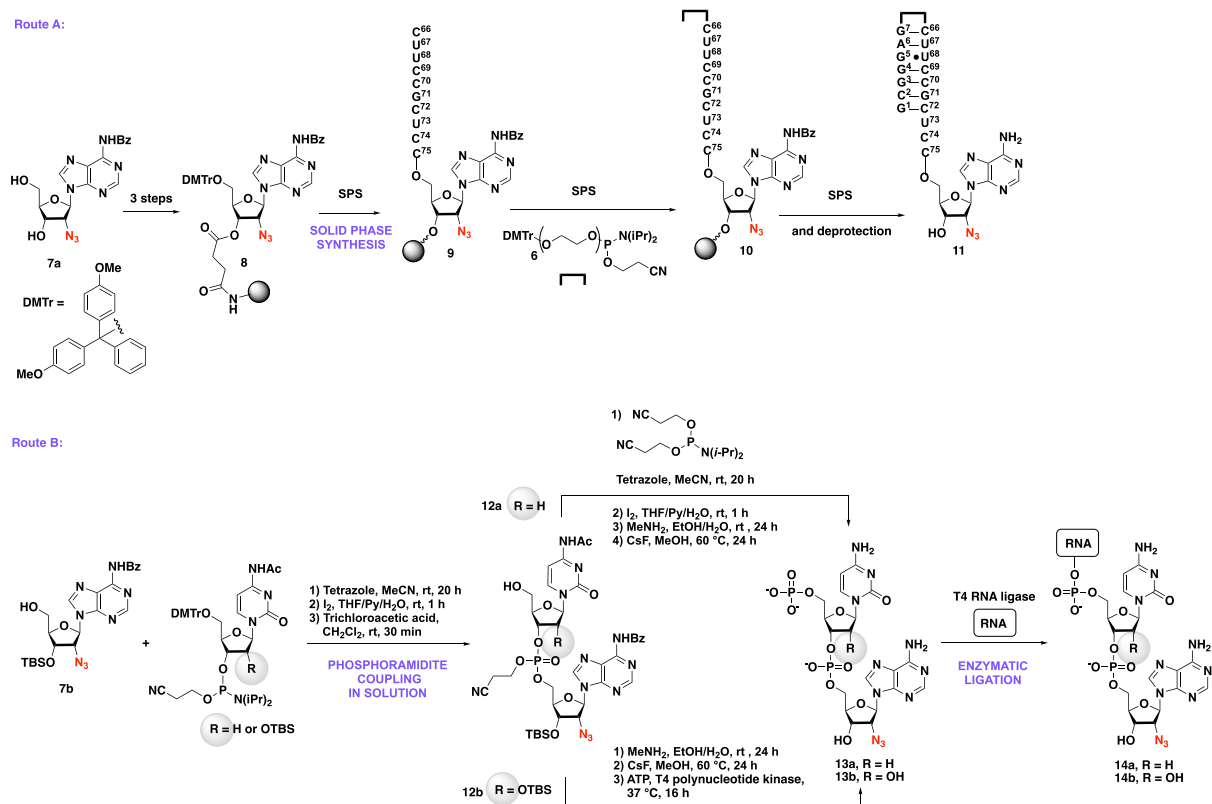
**13b**, respectively. Dinucleotides **13a–b** were then ligated to a 22-nt RNA helix in the presence of the T4 RNA ligase to produce the 24-nt azido-RNA helices **14a–b**. This chemoenzymatic strategy was also used to access full tRNA analogues of 76 nucleotides with a sequence corresponding to tRNA<sup>Ala</sup> [3], tRNA<sup>Gly</sup> [10], and tRNA<sup>Arg</sup> [13].

The second part of the bisubstrate structure, namely the peptide mimicking the growing peptidoglycan, was synthesized by semi-synthesis (Scheme 4). To access the peptidoglycan precursor containing an alkyne function **17**, meso-cystine was enzymatically incorporated into the peptidoglycan precursor providing compound **15** (Scheme 4). A reduction step in the presence of dithiothreitol (DTT) followed by the conversion of the L-Cys into dehydroalanine in the presence of *O*-(mesitylenesulfonyl)hydroxylamine (MSH) led to the formation of UDP–MurNac–pentapeptide **16** [8]. Finally, the addition of but-3-yne-1-thiol to the Michael acceptor produced alkyne-containing UDP–MurNac–pentapeptide **17**. The formation of the dehydroalanine into the peptide was optimized [5–7] by using 1,5-dibromohexanediamide instead of MSH in the presence of tris(2-carboxyethyl)phosphine (TCEP), providing a one-step process. Worthy of note, compound **17** is a mixture of diastereoisomers that were separated by HPLC purification.

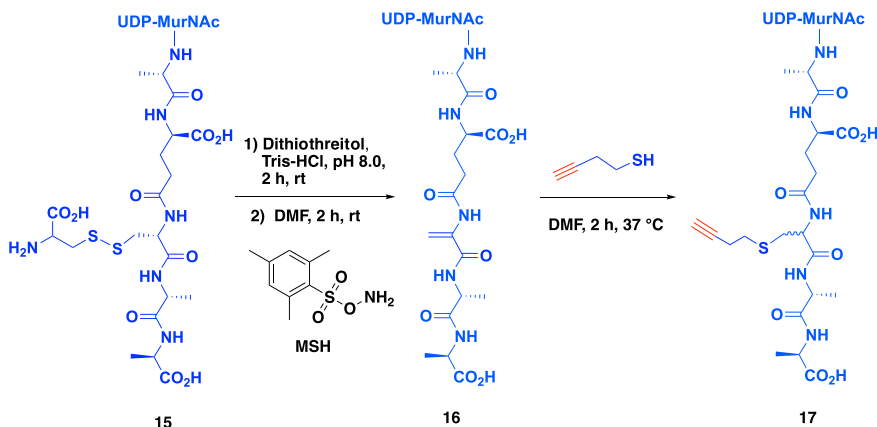
**Synthesis of peptidyl–RNA conjugates by CuAAC.** CuAAC is one of the most popular bioconjugation techniques reported in the past few decades for the late-stage modification of biomolecules. In 2013, the Etheve-Quellejeu group reported the use of this re-



**Scheme 2.** Synthesis of 2'-azido-2'-deoxyadenosine **7a** and **7b**.



**Scheme 3.** The two routes for the synthesis of 2'-azido-RNAs. Route A: synthesis of short azido-RNAs by SPS. Route B: synthesis of azido-RNA by a chemoenzymatic approach. DMTr protecting group is removed from the SPS machine.



**Scheme 4.** Synthesis of a peptidoglycan fragment containing a propargyl group.

action to access peptidyl–RNA conjugates as bisubstrates of Fem transferases.

The condition of the CuAAC reaction between 2'-azido-RNA **14a** and alkyne UDP–MurNAc–pentapeptide **17** has to be optimized first. Using azido-RNA helix **14a** (50 mM), alkyne peptide **17** (100 mM), copper sulfate (0.5 mM), sodium ascorbate (5 mM), and tris[(1-hydroxypropyl-1*H*-1,2,3-triazol-4-yl)methyl]amine (THPTA) (3.5 mM) in water for 24 h at 37 °C led to the expected peptidyl–RNA conjugate **18** in 36% yield after purification by denaturing polyacrylamide gel electrophoresis (Scheme 5A) [5]. The THPTA ligand was required to stabilize Cu(I) in aqueous buffer and avoid RNA degradation.

This versatile strategy was used in 2018 by Fonvielle *et al.* to access even more complex conjugates, namely lipid–carbohydrate–peptidyl–RNA conjugates **19** as bisubstrates of the transferase FmhB (Scheme 5B) [10].

### 2.2.2. Peptidyl–RNA conjugates with a squaramate linker

In 2016, Fonvielle *et al.* investigated the nature of the linker in bisubstrate compounds using a squarate motif to tether the RNA 3'-terminus and the peptide moiety. In this work, they described the introduction of a squaramide linkage by the reaction of 2'-amino-RNAs containing 4, 8, or 18 nucleotides with diethyl squarate diester followed by the reaction of the amino group of the lysine of the growing peptidoglycan peptide on the intermediate (Scheme 6) [14].

The synthesis starts with the reduction of the azido group of compounds **20a–c** in the presence of TCEP forming 2'-amino-RNA **21a–c**, which were then subjected to 1,4-addition with diethyl squarate diester to produce electrophilic RNA **22a–c** with yields ranging from 75% to 79%. The reaction of RNAs **22a–c** at pH 9.2 in the presence of UDP–MurNAc–pentapeptide **23** produced peptidyl–RNA conjugates with a squaramate linker in 23% to 45% yield. Importantly, increasing the size of the RNA moiety led to comparable reaction yields (Scheme 6). These results show that squarate-mediated ligation provides a versatile route to peptidyl–RNA conjugates. Significantly, this ligation is fully compatible with unprotected UDP–MurNAc–pentapeptide, which contains reactive functions such as phosphate, carbohydrate hydroxyl, and carboxyl groups.

### 2.2.3. Synthesis of peptidyl–XNA conjugates

In 2022, Rietmeyer *et al.* explored the nature of the RNA by reporting the synthesis of peptidyl–xeno-nucleic acid (XNA) conjugates to evaluate the impact of the incorporation of XNA into the acceptor arm of tRNA (Scheme 7) [15]. The bisubstrate molecules described in this study were composed of the following: (1) a peptidyl part, mimicking the UDP–MurNAc–pentapeptide, one of the substrates of Fem transferases; (2) an XNA part in which the riboses of RNA were replaced by 2'-deoxy-2'-fluororibose, 1',5'-anhydrohexitol, and 2'-deoxy-2'-fluoro-D-arabinose; and (3) a triazole linker. A series of 2'-azido-XNA **25a–j** were prepared and then subjected to CuAAC in







the RNA substrate were unsuccessful. In contrast, triazole-containing peptidyl–RNA or peptidyl–XNA conjugates enabled the successful crystallization of FemX<sub>Wv</sub> in complex with these conjugates [9,15].

In particular, the crystallographic structures of peptidyl–RNA conjugates in complex with the enzyme provide insights into the enzyme hot spots and catalytic mechanism. For instance, it has been demonstrated that the tetrahedral intermediate formed during catalysis is stabilized by Lys305 in FemX<sub>Wv</sub>. This enzyme creates a unique environment for substrate-assisted catalysis by orienting both Ala-tRNA<sup>Ala</sup> and UDP–MurNAc–pentapeptide into active conformations for aminoacyl transfer. This mechanism is unique to tRNA-dependent enzymes involved in protein-based peptide bond formation (Scheme 8) [9].

Structural data from peptidyl–XNA conjugates also revealed, for the first time, that the geometry of 1',5'-anhydrohexitol nucleotides closely resembles that of ribonucleotides, with the 1',5'-anhydrohexitol of hexitol nucleic acids mimicking ribose in its C-3'-endo sugar puckering. In contrast, the incorporation of 2'-deoxy-2'-fluoro-D-arabinose nucleic acids (2'F-ANA) and DNA residues into the single-stranded region resulted in the loss of a  $\pi$ -stacking interaction, leading to misalignment of the ACCA terminal moiety [15].

### 2.3.3. Conclusion

Collectively, these examples highlight the potential of peptidyl–RNA conjugates to explore non-ribosomal peptide synthesis, provide structural insights into RNA–enzyme interactions, and develop potent inhibitors.

## 3. Cofactor–RNA conjugates for the study of m<sup>6</sup>A methyltransferases

### 3.1. The m<sup>6</sup>A methyltransferases

The S-adenosyl-L-methionine (SAM) dependent methyltransferases (MTases) catalyze the transfer of a methyl group to their substrate using mainly the SAM cofactor as the methyl donor. This reaction leads to the release of the coproduct S-adenosyl-L-homocysteine (SAH) (Scheme 9). The MTases methylate several types of substrates including proteins, small molecules, and nucleic acids (DNA and

RNA) on which they are able to deposit this mark on different positions.

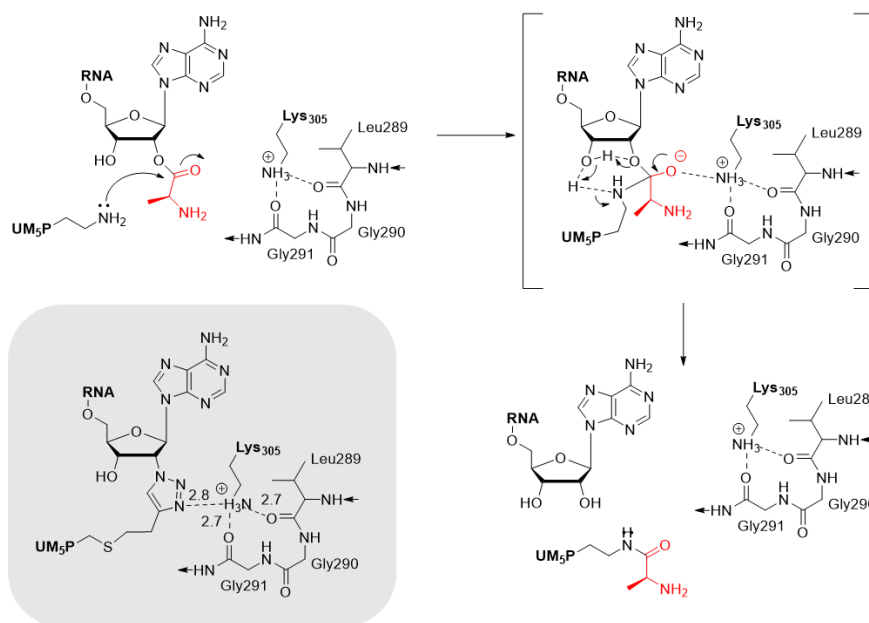
The installation of a methyl group is the most frequent modification found in RNA [17,18]. In particular, the introduction of a methyl group on the exocyclic N-6 atom of adenosine (m<sup>6</sup>A) by m<sup>6</sup>A MTases is the most studied epitranscriptomic mark, identified and characterized across all domains of life and all types of RNA [19]. The m<sup>6</sup>A modification has been shown to be essential in stabilizing RNA/RNA and RNA/protein interactions [20,21].

The m<sup>6</sup>A modification on mRNA is a dynamic and highly regulated process, involving three distinct families of proteins, that is, the writers (MTases) install the m<sup>6</sup>A mark, which is recognized by the reader proteins and removed by the erasers (Scheme 10). m<sup>6</sup>A is the most abundant internal modification in eukaryotic mRNA and long non-coding RNA [22,23]. It regulates different aspects of RNA metabolism such as splicing [24,25], stability [26], translation [27–29], and many more biological processes [30,31].

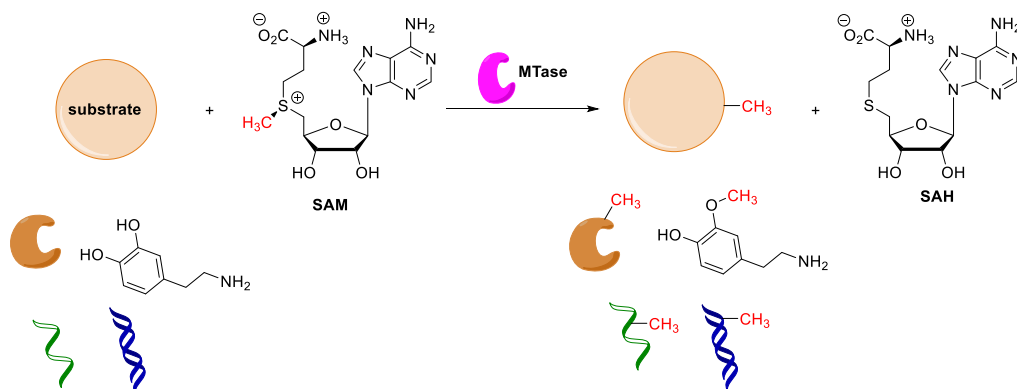
Importantly, it has been shown that dysregulation of MTase expression is correlated to human diseases including cancers [32–34], type 2 diabetes [35], neurological disorders [36], cardiovascular diseases [37], and viral infections [38,39].

Accumulating evidence indicates that m<sup>6</sup>A MTases are promising drug targets, and several pharmaceutical companies have already developed inhibitors of the METTL3/METTL14 complex. For example, STORM Therapeutics has announced the entry into Phase I of the selective METTL3 inhibitor STC-15 for the treatment of acute myeloid leukemia and solid tumors. An inhibitor of this enzyme complex identified by a fragment-based approach has also been reported by Gotham Therapeutics [40]. Very recently, the first inhibitors of METTL16 have been also described [41].

However, still little is known about the molecular mechanism of m<sup>6</sup>A modification, including the recognition of the RNA, which requires a sequence motif (DRACH, where A is the methylated adenosine; D=A, G, or U; R=A or G; and H=A, C, or U) and/or RNA structure, the binding in the active site of the MTase, and finally the release of the m<sup>6</sup>A substrate. This can be explained by difficulties encountered in obtaining RNA–protein crystallographic structures, leading to a limited number of structurally characterized m<sup>6</sup>A MTases. To date, only the catalytic domain



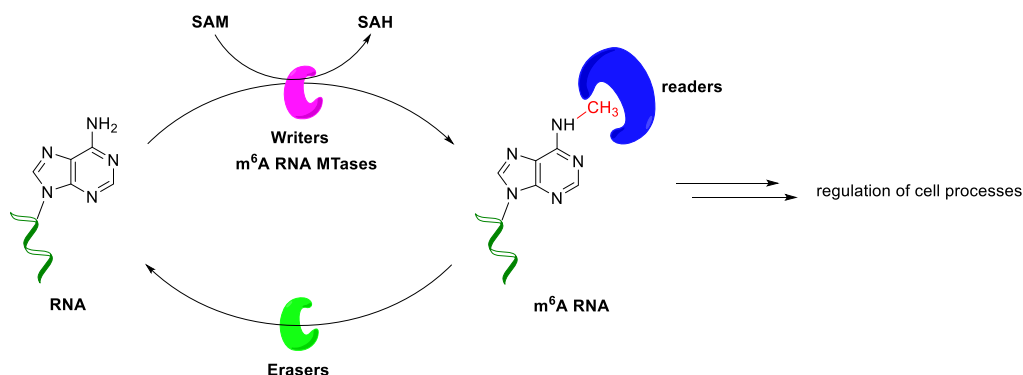
**Scheme 8.** Mechanism of the aminoacyl transfer catalyzed by FemX<sub>Wv</sub> [9].



**Scheme 9.** Methylation catalyzed by MTases.

of METTL16 has been crystallized with a substrate RNA [42], and no structure of the ternary complex has been reported. The structural studies carried out on human RNA MTases show that the substrate-binding site is largely open on the SAM-binding pocket, favoring the design of bisubstrate compounds [43]. In this context, bisubstrate analogues of MTases designed to accommodate the SAM-binding domain and the substrate-binding site appear as important chemical tools to access crystallographic structures that

would help in understanding better the enzymatic reaction. These compounds are SAM–adenosine and SAM–RNA conjugates, which contain an analogue of the cofactor SAM covalently attached to a substrate surrogate via an appropriate linker to mimic the transition state of the S<sub>N</sub>2 mechanism of the methylation reaction (Figure 3).



**Scheme 10.** The m<sup>6</sup>A modification process.

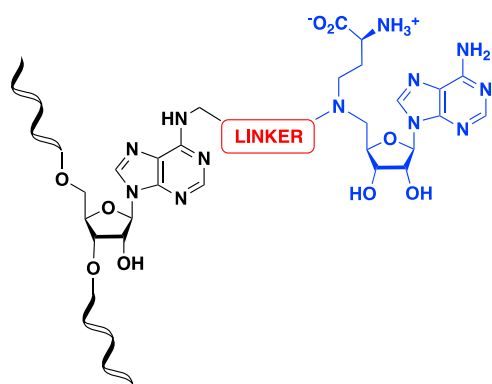


**Figure 3.** General structure of SAM-RNA conjugates.

### 3.2. Synthesis of SAM-adenosine and SAM-RNA conjugates

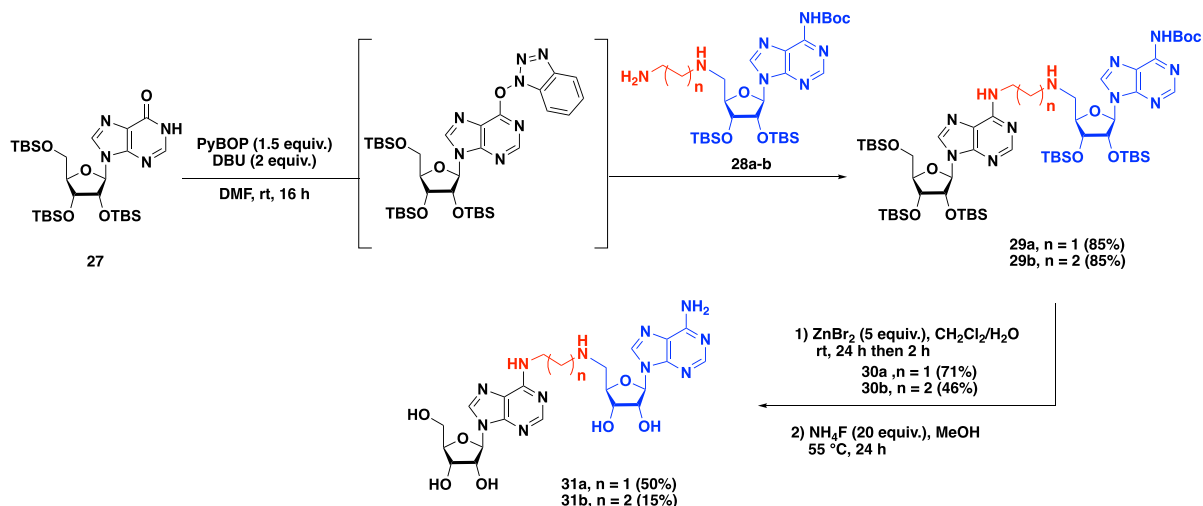
In respect of the bisubstrate strategy, Atdjian *et al.* reported in 2018 [44] a synthetic route to access SAM-adenosine conjugates. The structures of these compounds contain a SAM analogue covalently attached to a substrate surrogate via an alkyl linker that mimics the transition state of the S<sub>N</sub>2 mechanism of the methylation. The key step of the synthesis is based on the concept of the convertible nucleoside using the O<sup>6</sup>-(benzotriazol-1-yl)inosine [45–48] derivative as the electrophilic nucleoside to ensure the crucial connection between the SAM moiety bearing an alkyl linker and the N-6 position of the adenosine.

Bisubstrate molecules containing a SAM analogue with an alkyl linker **31a–b** were first synthesized

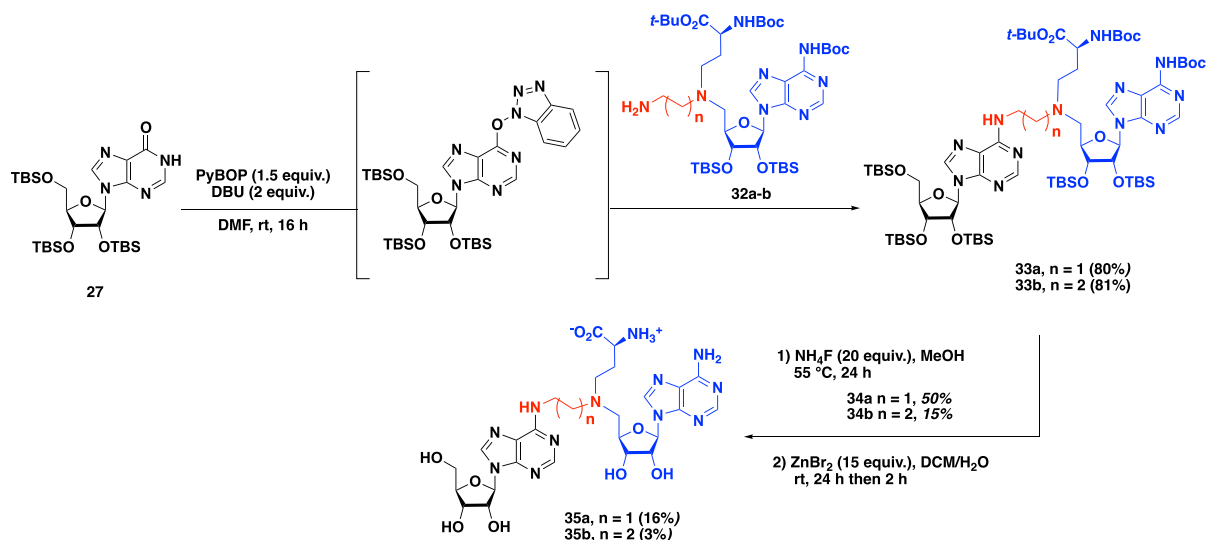
(Scheme 11) by Atdjian *et al.* [44]. Protected inosine **27** was activated *in situ* in the presence of PyBOP and DBU in DMF to generate the corresponding activated inosine intermediate, which was directly subjected to a nucleophilic aromatic substitution (S<sub>N</sub>Ar) with 5'-aminoadenosine derivatives **28a–b**, leading to the formation of SAM-adenosine conjugates **29a** and **29b** in 85% yield. The removal of the protecting groups was then achieved using ZnBr<sub>2</sub> salt, yielding **30a** and **30b** in 71% and 46%, respectively. Treatment with ammonium fluoride gave access to the fully deprotected bisubstrates **31a** and **31b**.

To ensure better affinity with methyltransferase, a second generation of SAM-adenosine conjugates with an alkyl linker was prepared in which an  $\alpha$ -amino-acid motif mimicking the  $\alpha$ -amino-acid side chain of the cofactor SAM was introduced [44]. The convertible nucleoside approach was used in the presence of adenosine derivatives **32a–b** substituted at the C-5' position by an  $\alpha$ -amino-acid residue and an alkyl linker containing two to three carbon atoms to access compounds **33a** and **33b** in 80% and 81% yield, respectively. A two-step procedure was applied to remove the protecting groups of the adenosine analogues and the  $\alpha$ -amino-acid side chain, leading to the formation of bisubstrate molecules **35a** and **35b** (Scheme 12).

To increase the size of the part mimicking the RNA substrate, Etheve-Quellejeu and coworkers applied the convertible nucleoside strategy to short RNA strands [49]. Activated inosine **36** was subjected to a phosphoramidite coupling in the presence of the commercially available guanosine phospho-



**Scheme 11.** Synthesis of adenosine–SAM bisubstrates containing an alkyl linker by a convertible nucleoside approach.

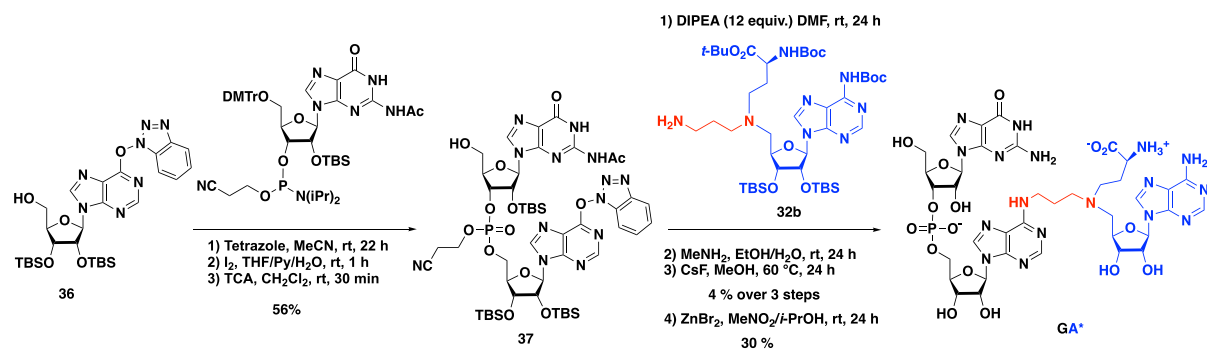


**Scheme 12.** Synthesis of SAM–adenosine bisubstrates containing an alkyl linker and  $\alpha$ -amino-acid side chain.

ramidite and tetrazole in acetonitrile. The triester phosphite intermediate was then oxidized with a solution of diiodine in a water/THF/pyridine mixture to access the corresponding phosphotriester. Deprotection of the C-5' position was carried out by treatment with trichloroacetic acid in order to remove the 4,4'-dimethoxytrityl group. Dinucleotide **37** was thus obtained in three steps in 56% yield (Scheme 13).

The S<sub>N</sub>Ar reaction with SAM analogue **32b** followed by three deprotection steps finally yielded the dinucleotide **GA\***.

The introduction of the SAM analogue in internal position requires the preparation of the convertible phosphoramidite derivative **33**, in which the N-6 position is activated with an *O*<sup>6</sup>-(benzotriazol-1-yl) group in six steps starting from inosine (Scheme 14).



**Scheme 13.** Synthesis of **GA\*** dinucleotide–SAM conjugate.

The **A\*A** dinucleotide– and the **GA\*A** trinucleotide–SAM conjugates were obtained following the phosphoramidite coupling strategy described above [49].

The synthesis of a SAM–RNA conjugate with a longer RNA strand was then performed by a chemoenzymatic strategy [49]. An enzymatic ligation catalyzed by the T4 RNA ligase was used to link a dinucleotide covalently tethered to the SAM analogue (**pdGA\***) to a synthetic 11-nt RNA molecule to produce the corresponding 13-nt SAM–RNA conjugate (Scheme 15).

Urea was also chosen to provide bisubstrates with a linker containing only one carbon atom as in the  $S_N2$  mechanism of the methyl transfer catalyzed by the MTases [44]. To synthesize such molecules, the exocyclic amine at the N-6 position of adenosine **34** was first activated with *isopropenyl* chloroformate to access the corresponding *isopropenyl* carbamate **35** in 75% yield (Scheme 16). Then, the condensation with secondary amine **36** in pyridine produced urea **37** in 85% yield. The deprotection of the silyl groups with  $NH_4F$  followed by the removal of the Boc groups and *tert*-butyl ester allowed the formation of urea bisubstrate **38** in 47% yield.

Moving forward to explore the impact of the linker of the SAM–adenosine conjugates, Atdjian *et al.* [50] examined in 2020 the CuAAC reaction to introduce 1,4-disubstituted-triazole ring as a linker (Scheme 17). The CuAAC reaction between N-6-propargyl adenosine **39** and 5'-azido-adenosine **40** was conducted in the presence of sodium ascorbate and copper sulfate in DMF/ $H_2O$  to obtain triazole bisubstrate **41** in 36% yield (Scheme 17). Interestingly, this approach, allowing the formation of a 1,2,3-triazole link between the adenosine and the

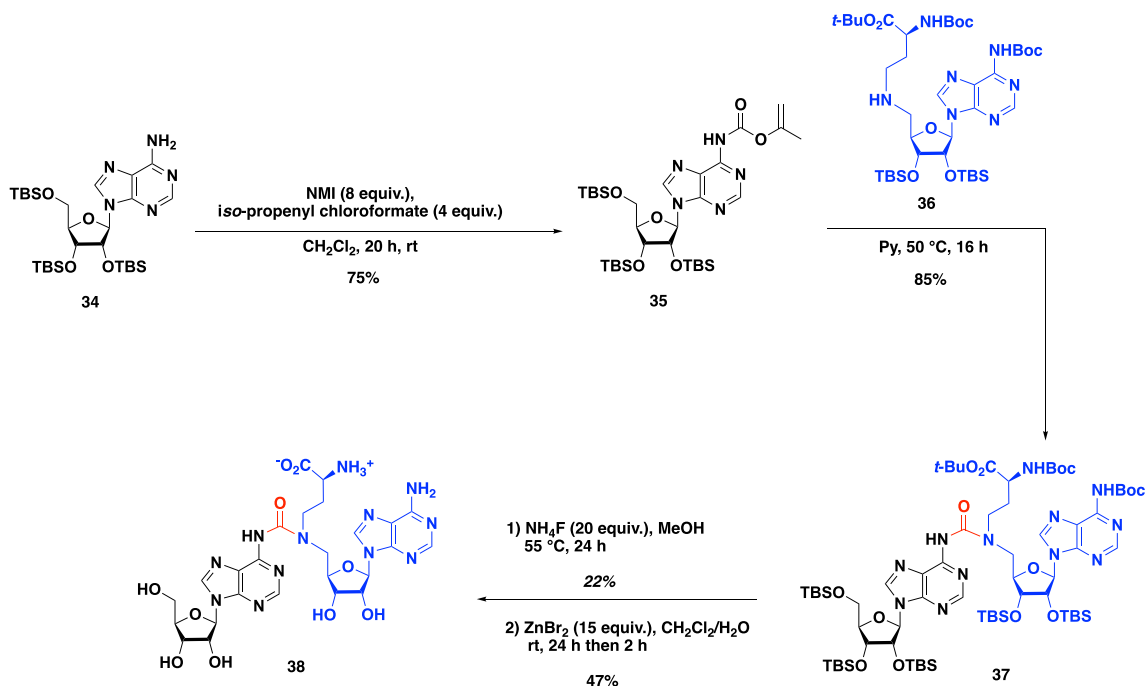
SAM analogue, does not require any protecting group on the reactive functions of the nucleosides.

In addition to their effort to access the SAM–adenosine conjugate connected at the N-6 position, Etheve-Quellejeu and coworkers explored in the same year [50] the reactivity of the N-1 position of adenosine to prepare bisubstrate molecules to study  $m^1A$  MTase. The synthesis of SAM–adenosine conjugate **43** with a triazole linker connected at the N-1 position was achieved by the CuAAC between N-1 propargyl adenosine derivative **42** and 5'-azido-adenosine **40**. In the presence of sodium ascorbate and copper sulfate, the expected positively charged conjugate **43** was isolated in 53% yield (Scheme 17).

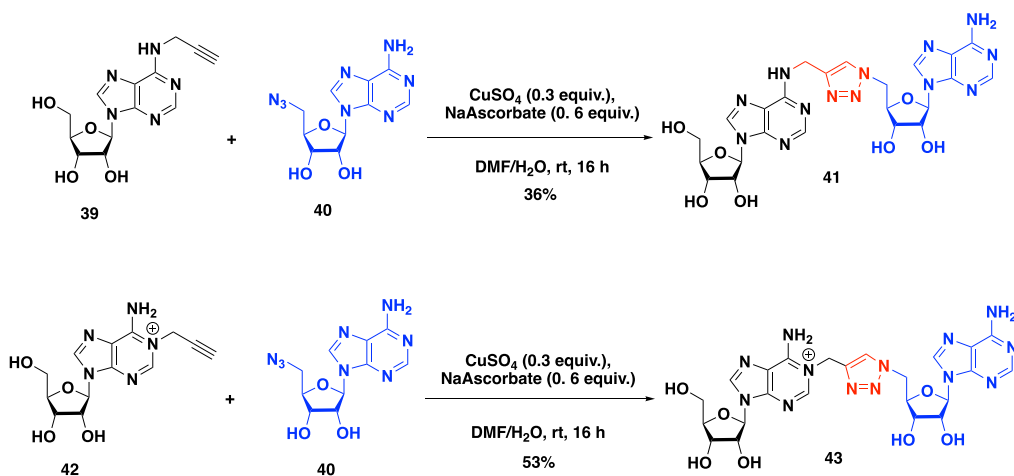
As seen above, CuAAC efficiently provides bisubstrate analogues with a 1,2,3-triazole linker. However, this strategy does not allow the introduction of the  $\alpha$ -amino-acid motif of the SAM cofactor. To overcome this issue, Coelho *et al.* developed in 2023 a two-step metal-catalyzed procedure to access bisubstrate analogues of RNA MTase [51]. In this work, 5-iodotriazole was modified by metal-catalyzed reactions. The reactivity of adenosine derivatives in iodo copper(I) azide–alkyne cycloaddition (iCuAAC) reaction was achieved between adenosine **39** substituted at the N-6 position with an alkyne function and 5'-azido-adenosine **40**. The 5-iodotriazole compound **44** was obtained in 38% yield in the presence of a substoichiometric amount of  $Cu(ClO_4)_2$ , an excess of NaI as the iodinating source, *N,N*-diisopropylethylamine (DIPEA), and tris(benzyltriazolylmethyl)amine as the ligand in DMF (Scheme 18).

A second metal-catalyzed promoted reaction was optimized to introduce the  $\alpha$ -amino-acid motif

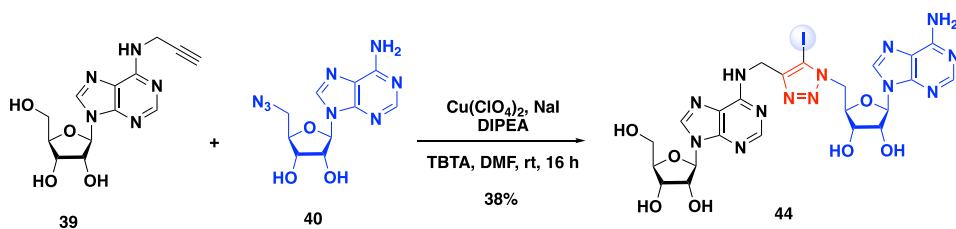




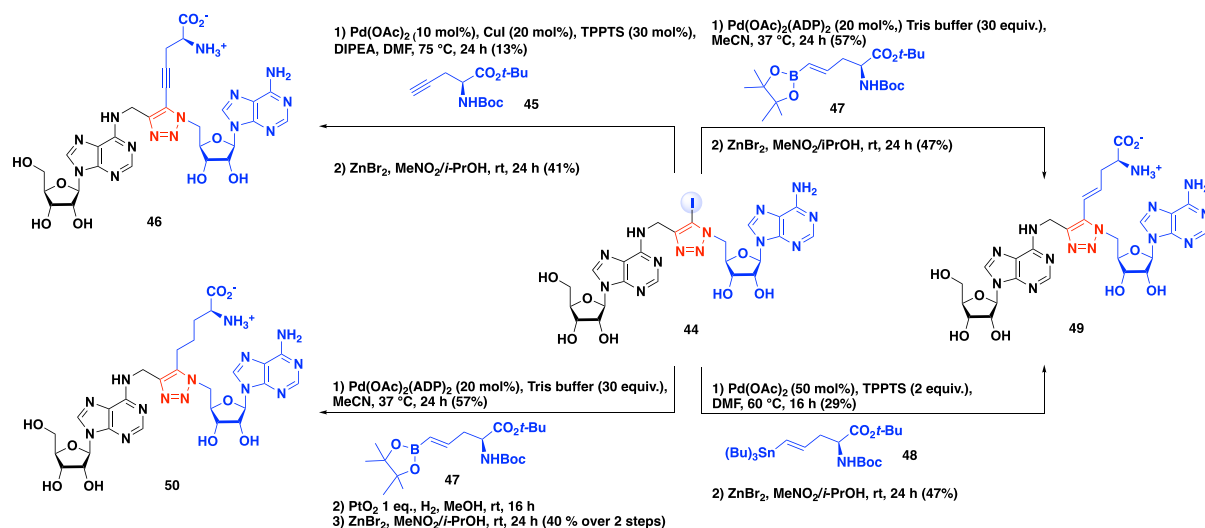
**Scheme 16.** Synthesis of a SAM–adenosine conjugate with a urea linker.



**Scheme 17.** Synthesis of N-6 and N-1 SAM–adenosine conjugates by CuAAC.



**Scheme 18.** Synthesis of 5-iodotriazole compound 44 by iCuAAC.



**Scheme 19.** Functionalization of 5-iodotriazole **44** by metal-catalyzed cross-coupling.

the N-6 position of the adenosine during oligonucleotide synthesis. The resulting propargyl-N-6-A-RNA **51** was then subjected to iCuAAC in the presence of 5'-azido-adenosine **52** to form 5-iodotriazole derivative **53**. A second step of late-stage modification of the SAM-RNA conjugate, in the presence of pinacolboronic ester **47**, followed by the removal of *tert*-butyl and Boc protecting groups led to the formation of bisubstrate analogue **54** containing a SAM analogue covalently attached to the RNA substrate via a 1,2,3-triazole linker substituted at the C-5 position with an  $\alpha$ -amino-acid motif (Scheme 20).

### 3.3. Biological results

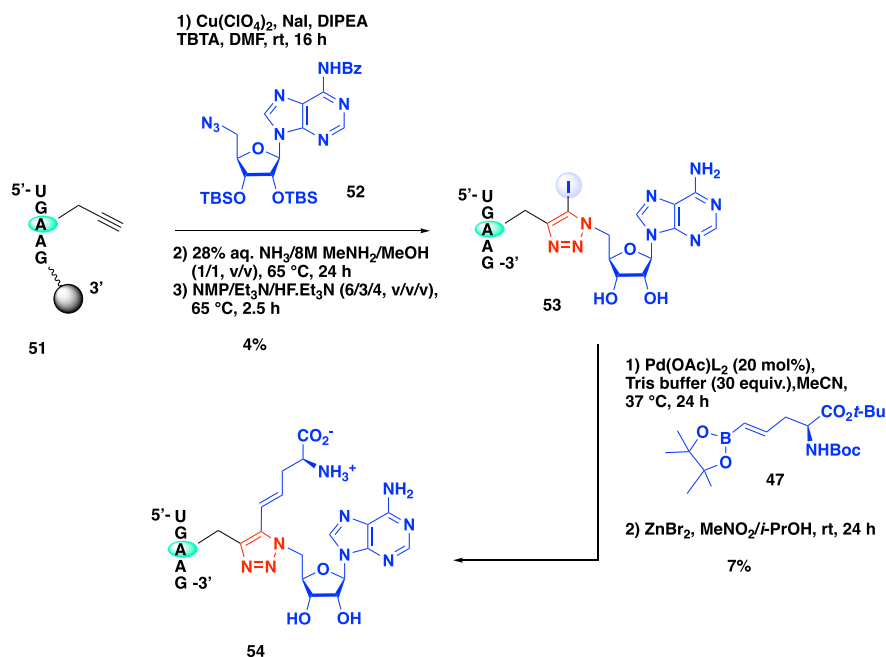
The SAM-adenosine conjugates were evaluated on the bacterial rRNA MTase RlmJ, which methylates the 23S rRNA at position A2030 and on METTL3-14, which deposits the m<sup>6</sup>A mark on human mRNA. This enzymatic complex is involved in human diseases and considered a promising drug target [32,35,38].

The binding of SAM-adenosine conjugates **31a-b**, **35a-b**, and **38** to RlmJ was first assayed using differential scanning fluorimetry [52]. Compounds **31a-b** show an increase in the T<sub>m</sub> value, indicating that they establish stabilizing interactions with the protein compared to other potential bisubstrates.

This result also underlines the importance of the methionine part of the SAM analogue likely to be involved in the interaction and an aliphatic linker. In addition, compounds **35a** and **35b** display K<sub>D</sub> values of 25 and 30  $\mu$ M, respectively. X-ray structures were solved for the complexes **35a**/RlmJ and **35b**/RlmJ. In the complex **35b**/RlmJ, one structure shows that the RNA moiety of the conjugate binds the presumed substrate pocket of the enzyme while the cofactor analogue occupies partly the SAM-binding site, showing a rotation of 120° of the adenosine out of the pocket (Figure 4A). Importantly, compound **35b** interacts with key residues involved in the catalytic mechanism, and the crystallographic structure confirms the interactions of the methionine part with the active site (Figure 4B). All together, these results indicate that the positioning of conjugate **35b** in RlmJ resembles the transition state of the S<sub>N</sub>2 mechanism of the methyl transfer.

In order to fully decipher the mechanism of methylation catalyzed by METTL3-14, conjugates **35a-b** were also used as tools in a combined experimental and computational approach [53]. First, the inhibitory potency of the compounds was determined using a reader-based TR-FRET assay. Under these conditions, the conjugates exhibit IC<sub>50</sub> values in the low micromolar range. Several crystallographic structures of METTL3-14 in complex with compounds **35a-b** were solved. Analysis of the





**Scheme 20.** Synthesis of SAM–RNA conjugate **54** with a triazole linker substituted by an analogue of the methionine side chain.

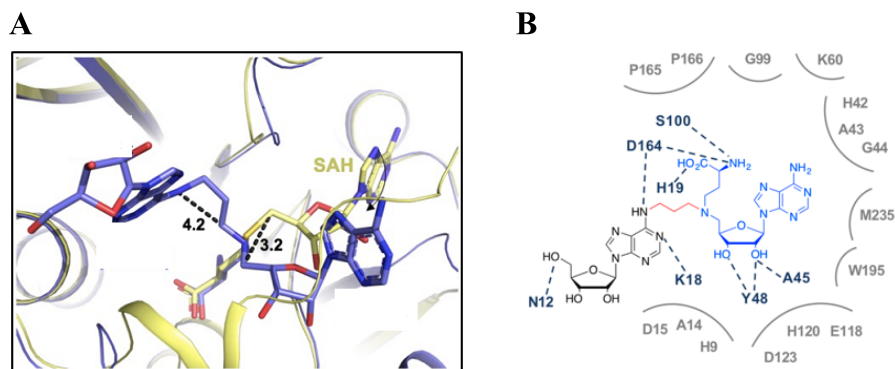


**Figure 4.** (A) Structure of **35b**/RlmJ (blue) aligned with SAH/RlmJ (yellow) [52]. (B) Interaction map of bisubstrate **35b** in the active site of RlmJ [52].

interaction networks between the active site and the conjugates validated their use as tools to decipher the catalytic mechanism. In particular, compound **35a** was identified as the transition state analogue of the methyl transfer catalyzed by METTL3. Using the crystal structure of the complex **35a**–METTL3–14 (Figure 5), QM/MM simulations allowed for the proposition of the mechanism catalyzed by METTL3–14.

To go further, SAM–RNA conjugates with in-

creased size of the RNA part were also used in crystallization assays with RlmJ to gain insights into the m<sup>6</sup>A methylation process [49]. Two crystallographic structures were obtained with SAM–RNA conjugates **GA\*** and **GA\*A** containing a dinucleotide and a trinucleotide as the substrate, respectively. In the case of the dinucleotide **GA\***, the adenosine of the SAM analogue shows a correct orientation in the SAM pocket. All together, these two RX structures allowed for the construction of a model showing the

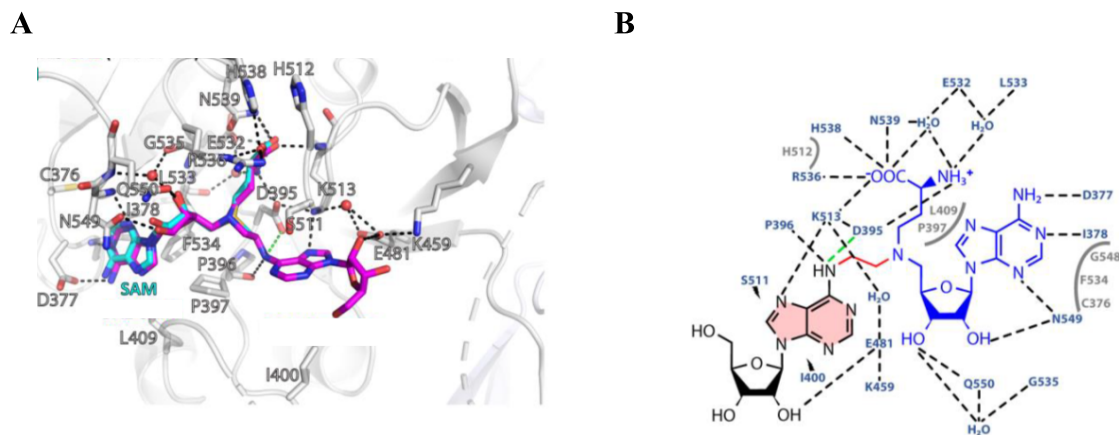


**Figure 5.** (A) Superposition of the crystal structure of METTL3–14 bound to **35a** (magenta) and SAM (blue) [53]. (B) Interaction map of bisubstrate **35a** in the active site of METTL3–14 [53].

SAM cofactor and a trinucleotide with the sequence GA<sup>2030</sup>A of *E. coli* 23S rRNA bound to RlmJ. Thanks to this model, we were able to propose a mechanism for the methylation reaction catalyzed by RlmJ (Scheme 21) [49].

In summary, the SAM–adenosine conjugates are valuable tools to decipher the full mechanism of other RNA MTases and also for the design of potent inhibitors.

#### 4. Conclusion and outlook

The chemical approaches discussed in this review highlight the versatility and efficiency of nucleoside and nucleotide chemistry in addition to SPS and the chemoenzymatic approach in the design of RNA conjugates for the study of RNA transferases. These methods allow for significant flexibility in modifying the bisubstrate compounds, including the RNA sequence and size, the nature of the linkers, and the peptide or cofactor components. Such adaptability is crucial for tailoring these chemical tools to explore a wide range of transferases beyond the examples provided in this work, extending their utility to new classes of RNA-dependent enzymes.

The insights they provide into enzyme–substrate interactions are particularly valuable not only for fundamental research in RNA biology but also for drug discovery. Indeed, since new transferases continue to be discovered and considered as promising new drug targets [54], these chemical tools will be instrumental in the development of new therapeutic strategies.

#### Declaration of interests

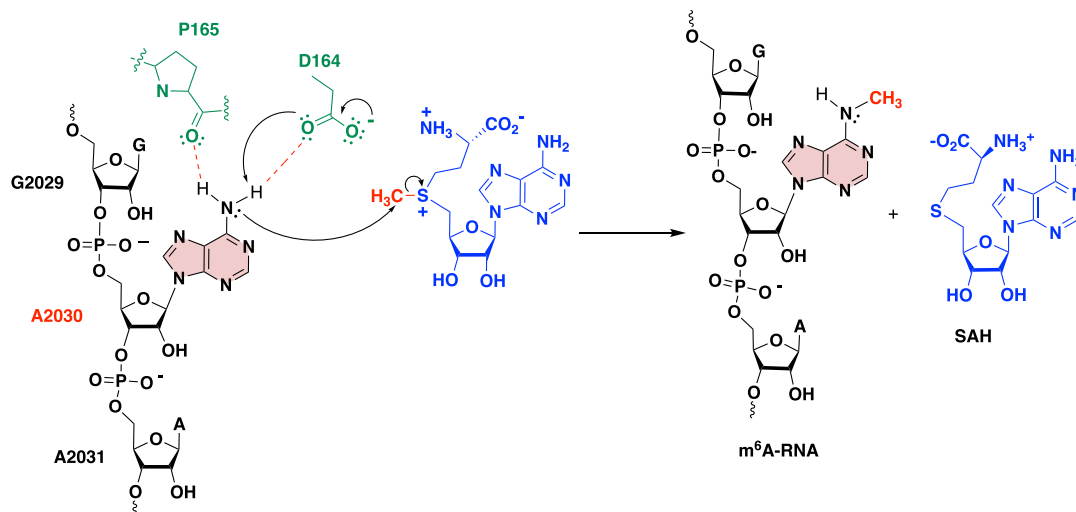
The authors do not work for, advise, own shares in, or receive funds from any organization that could benefit from this article, and have declared no affiliations other than their research organizations.

#### Funding

The authors thank the CNRS and Paris Cité University for their support and the Agence Nationale de la Recherche (ANR: ARNTools, SyntRNA) and La Ligue contre le Cancer for funding.

#### References

- [1] R. Ahmed-Belkace, F. Debart and J.-J. Vasseur, *Eur. J. Org. Chem.* **21** (2022), article no. e202101481.
- [2] A. Bouhss, N. Josseaume, D. Allanic, et al., *J. Bacteriol.* **183** (2001), pp. 5122–5127.
- [3] S. S. Hegde and T. E. Shrader, *J. Biol. Chem.* **276** (2001), pp. 6998–7003.
- [4] K. Dare and M. Ibba, *WIREs RNA* **3** (2012), pp. 247–264.
- [5] M. Chemama, M. Fonvielle, M. Arthur, J. M. Valery and M. Etheve-Quellejeu, *Chem. Eur. J.* **15** (2009), pp. 1929–1938.
- [6] M. Chemama, M. Fonvielle, R. Villet, M. Arthur, J. M. Valery and M. Etheve-Quellejeu, *J. Am. Chem. Soc.* **129** (2007), pp. 12642–12643.
- [7] E. Cressina, A. J. Lloyd, G. De Pascale, B. J. Mok, S. Caddick, D. I. Roper, C. G. Dowson and T. D. H. Bugg, *Bioorg. Med. Chem.* **17** (2009), pp. 3443–3455.
- [8] M. Fonvielle, D. Mellal, D. Patin, et al., *Chem. Eur. J.* **19** (2013), pp. 1357–1363.
- [9] M. Fonvielle, I. Li de la Sierra-Gallay, A. El-Sagheer, et al., *Angew. Chem. Int. Ed.* **125** (2013), pp. 7419–7422.



**Scheme 21.** Proposed mechanism for the methylation reaction catalyzed by RlmJ [49].

- [10] M. Fonvielle, A. Bouhss, C. Hoareau, et al., *Chem. Eur. J.* **24** (2018), pp. 14911–14915.
- [11] M. Fonvielle, M. Chemama, M. Lecerf, R. Villet, P. Busca, A. Bouhss, M. Etheve-Quellejeu and M. Arthur, *Angew. Chem. Int. Ed.* **49** (2010), pp. 5115–5119.
- [12] C. Kitoun, S. Saidjalolov, D. Bouquet, et al., *ACS Omega* **8** (2023), pp. 3850–3860.
- [13] Y. Afandizada, T. Abeywansa, V. Guerineau, Y. Zhang, B. Sargueil, L. Ponchon, L. Iannazzo and M. Etheve-Quellejeu, *Methods* **229** (2024), pp. 94–107.
- [14] M. Fonvielle, N. Sakkas, L. Iannazzo, et al., *Angew. Chem. Int. Ed.* **55** (2016), pp. 13553–13557.
- [15] L. Rietmeyer, I. de la Sierra-Gallay, G. Schepers, et al., *Nucleic Acids Res.* **50** (2022), pp. 11415–11425.
- [16] S. Biarrotte-Sorin, A. P. Maillard, J. Delettré, W. Sougakoff, M. Arthur and C. Mayer, *Structure* **12** (2004), pp. 257–267.
- [17] Y. Motorin and M. Helm, *WIREs RNA* **13** (2022), article no. e1691.
- [18] P. Boccaletto, F. Stefaniak, A. Ray, et al., *Nucleic Acids Res.* **50** (2022), pp. D231–D235.
- [19] M. Frye, S. R. Jaffrey, T. Pan, G. Rechavi and T. Suzuki, *Nat. Rev. Genet.* **17** (2016), pp. 365–372.
- [20] P. V. Sergiev, A. Y. Golovina, I. A. Osterman, et al., *J. Mol. Biol.* **428** (2016), pp. 2134–2145.
- [21] J. Huang and P. Yin, *Genom. Proteom. Bioinform.* **16** (2018), pp. 85–98.
- [22] D. Dominissini, S. Moshitch-Moshkovitz, M. Salmon-Divon, N. Amariglio and G. Rechavi, *Nat. Protocols* **8** (2013), pp. 176–189.
- [23] K. D. Meyer, Y. Saletore, P. Zumbo, O. Elemento, C. E. Mason and S. R. Jaffrey, *Cell* **149** (2012), pp. 1635–1646.
- [24] W. Xiao, S. Adhikari, U. Dahal, et al., *Cell* **61** (2016), pp. 507–519.
- [25] X. Zhao, Y. Yang, B.-F. Sun, et al., *Cell Res.* **24** (2014), pp. 1403–1419.
- [26] X. Wang, Z. Lu, A. Gomez, et al., *Nature* **505** (2014), pp. 117–120.
- [27] K. D. Meyer, D. P. Patil, J. Zhou, et al., *Cell* **163** (2015), pp. 999–1010.
- [28] J. Zhou, J. Wan, X. Gao, X. Zhang, S. R. Jaffrey and S.-B. Qian, *Nature* **526** (2015), pp. 591–594.
- [29] X. Wang, B. S. Zhao, I. A. Roundtree, et al., *Cell* **161** (2015), pp. 1388–1399.
- [30] G. Cao, H. B. Li, Z. Yin and R. A. Flavell, *Open Biol.* **6** (2016), article no. 160003.
- [31] Z. M. Zhu, F. C. Huo and D. S. Pei, *Int. J. Biol. Sci.* **16** (2020), pp. 1929–1940.
- [32] R. Gao, M. Ye, B. Liu, M. Wei, D. Ma and K. Dong, *Front. Oncol.* **11** (2021), article no. 679367.
- [33] W. Zhao, X. Qi, L. Liu, S. Ma, J. Liu and J. Wu, *Mol. Ther. Nucleic Acids* **19** (2020), pp. 405–412.
- [34] I. Barbieri and T. Kouzarides, *Nat. Rev. Cancer* **20** (2020), pp. 303–322.
- [35] D. F. De Jesus, Z. Zhang, S. Kahraman, et al., *Nat. Metab.* **1** (2019), pp. 765–774.
- [36] B. Chatterjee, C.-K. J. Shen and P. Majumder, *Int. J. Mol. Sci.* **22** (2021), article no. 11870.
- [37] L. Dorn, S. Tual-Chalot, K. Stellos and F. Accornero, *J. Mol. Cell Cardiol.* **129** (2019), pp. 272–280.
- [38] W. Dang, Y. Xie, P. Cao, S. Xin, J. Wang, S. Li, Y. Li and J. Lu, *Front. Microbiol.* **10** (2019), article no. 417.
- [39] G. D. Williams, N. S. Gokhale and S. M. Horner, *Annu. Rev. Virol.* **6** (2019), pp. 235–253.
- [40] M. Berdasco and M. Esteller, *Br. J. Pharmacol.* **179** (2022), pp. 2868–2889.
- [41] Y. Liu, G. L. Goebel, L. Kanis, O. Hastürk, C. Kemker and P. Wu, *J. Am. Chem. Soc. Au* **4** (2024), pp. 1436–1449.
- [42] K. A. Doxtader, P. Wang, A. M. Scarborough, D. Seo, N. K. Conrad and Y. Nam, *Mol. Cell* **71** (2018), pp. 1001–1011.
- [43] M. Schapira, *ACS Chem. Biol.* **11** (2016), pp. 575–582.

- [44] C. Atdjian, L. Iannazzo, E. Braud and M. Ethève-Quellejeu, *Eur. J. Org. Chem.* **2018** (2018), pp. 4411–4425.
- [45] S. Bae and M. K. Lakshman, *J. Am. Chem. Soc.* **129** (2007), pp. 782–789.
- [46] W. Hong and J. Dowden, *Chin. Chem. Lett.* **22** (2011), pp. 1439–1442.
- [47] Z. K. Wan, S. Wacharasindhu, C. G. Levins, M. Lin, K. Tabei and T. S. Mansour, *J. Org. Chem.* **72** (2007), pp. 10194–10210.
- [48] M. Ramadan, N. K. Bremner-Hay, S. A. Carlson and L. R. Comstock, *Tetrahedron* **70** (2014), pp. 5291–5297.
- [49] V. Meynier, L. Iannazzo, M. Catala, *et al.*, *Nucleic Acids Res.* **50** (2022), pp. 5793–5806.
- [50] C. Atdjian, D. Coelho, L. Iannazzo, M. Ethève-Quellejeu and E. Braud, *Molecules* **25** (2020), article no. 3241.
- [51] D. Coelho, L. Le Corre, K. Bartosik, L. Iannazzo, E. Braud and M. Ethève-Quellejeu, *Chem. Eur. J.* **29** (2023), article no. e202301134.
- [52] S. Oerum, M. Catala, C. Atdjian, *et al.*, *RNA Biol.* **16** (2019), pp. 798–808.
- [53] I. Corbeski, P. A. Vargas-Rosales, R. K. Bedi, *et al.*, *eLife* **12** (2023), article no. RP9253.
- [54] F. Fiorentino, M. Menna, D. Rotili, S. Valente and A. Mai, *J. Med. Chem.* **66** (2023), pp. 1654–1677.